WWW.IJRPR.COM

International Journal of Research Publication and Reviews

Journal homepage: www.ijrpr.com ISSN 2582-7421

Enhancement and Validation of the Latest Solid-State Peltier Thermoelectric System Model for Sterilization and Freezing Operations in Ambulances

Sasikumar K[1], Velmurugan K[2]

[1]*Assistant Professor, Department of Electrical and Electronics Engineerin, Panimalar Engineering College, Chennai, Tamil Nadu 600123*
[2]*Assistant Professor, Vels School of Maritime Studies, Chennai, Tamil Nadu 603103*
DOI: https://doi.org/10.55248/gengpi.4.723.49834

A B S T R A C T

In this paper, the latest model of a solid-state Peltier thermoelectric system was thoroughly reviewed and improved. A heating-cooling chamber was specifically designed and fabricated using Peltier modules. The equivalent circuit of the system was extracted and simulated. The main objective was to implement this advanced thermoelectric system in ambulances for sterilization and freezing operations. To validate the effectiveness of the model, comprehensive experimental tests were conducted on the overall system. Furthermore, Spice simulations were performed to compare and verify the simulation outcomes with the experimental results. The simulation results exhibited a high degree of compatibility with the experimental findings, confirming the accuracy of the model. This validated model can be easily adapted for other Peltier-based thermoelectric devices, allowing for the simulation of various thermoelectric systems based on similar modules. Its successful implementation in ambulances for sterilization and freezing operations holds promising potential for future applications in the medical field.

Keywords: Thermoelectric cooler, thermoelectric generator, thermoelectric module, coefficient of performance, SPICE model.

1. INTRODUCTION

At the core of thermoelectric (TE) technology lies the intriguing Peltier effect, initially observed in the early 19th century. This remarkable phenomenon occurs when an electric current passes through dissimilar conductors. Remarkably, the junction of these conductors will either absorb or release heat, contingent on the direction of the current flow. Comprehending the intricacies of the Peltier effect and its operation in thermoelectric devices presents a formidable challenge. However, exploring this phenomenon is essential to grasp the underlying principles that drive the functioning of modern thermoelectric gadgets. The development of thermoelectric materials has seen a significant breakthrough with the implementation of n-type and p-type semiconductor materials. By precisely controlling the carrier concentration, the optimization of the bandgap can be achieved, enhancing the efficiency of the thermoelectric couple.

To harness the full potential of these materials, numerous thermocouples are interconnected electrically in series, leading to an increased operating voltage. Simultaneously, they are connected thermally in parallel, thereby enhancing the overall thermal conductivity. This arrangement results in the formation of a thermoelectric module (TEM). TEM devices can be broadly categorized into two types: thermoelectric generators (TEGs) and thermoelectric coolers (TECs). TEGs are designed to convert heat energy into electrical power, while TECs aim to transfer heat from one side of the module to the other when an electrical current is applied. By leveraging these advancements, thermoelectric technology continues to pave the way for numerous applications in power generation and temperature control systems, promising a greener and more efficient future. Thermoelectric generators (TEGs) harness the Seebeck effect to convert thermal power from a temperature gradient into electric power. On the other hand, thermoelectric coolers (TECs) leverage the Peltier effect to convert electric power into a temperature gradient. These devices are solid-state power converters, devoid of mechanical and moving parts, offering numerous advantages such as noiselessness, compactness, reliability, and stability. One of the key benefits of TEGs and TECs is their ability to operate without noise or vibrations, making them suitable for applications where quiet and precise operation is essential. Additionally, their compact size and solid-state nature make them highly reliable, as there are no components prone to wear or failure. Despite these advantages, both TEGs and TECs have historically suffered from relatively poor energy conversion efficiency, limiting their widespread adoption in mainstream applications. As a result, they have been primarily employed in niche applications where their unique advantages outweigh their lower efficiency. However, ongoing research and advancements in thermoelectric materials and design have shown promising potential for improving the efficiency of these devices. With further improvements, thermoelectric technology may find broader applications in the future, offering environmentally friendly and efficient solutions in various industries.

Thermoelectric Coolers (TECs) are well-suited for cooling and refrigeration purposes, finding applications in specialized coolers for optoelectronic and electronic components, as well as portable electric food coolers and heaters. They excel in scenarios where precise temperature control is essential, offering attributes such as accuracy, simplicity, reliability, and compactness. These qualities make them highly suitable for various industries, including electronics, food preservation, and medical equipment. On the other hand, Thermoelectric Generators (TEGs) are primarily used to harness waste heat from sources with available temperature differences and convert it into electric power. They have found significant applications in power generation for spacecraft systems and serve as thermocouples for temperature measurement. With the escalating costs of fossil fuels and increasing emphasis on waste-heat recovery, TEG devices are gaining prominence in broader automotive systems and remote self-powered sensor and wireless communication systems.

TEGs have the potential to play a crucial role in sustainable energy solutions, particularly in scenarios where waste heat can be harnessed and converted into usable electricity. As environmental concerns continue to grow, the development and adoption of TEGs are expected to increase, contributing to the advancement of greener and more energy-efficient technologies.

The mathematical models of Thermoelectric Modules (TEMs) for both Thermoelectric Coolers (TECs) and Thermoelectric Generators (TEGs) have been extensively developed to simulate their respective behaviors and analyze their performance [1, 2]. These models enable the analysis, design, and optimization of TEMs, significantly reducing the design cycle time. In recent times, equivalent circuit models of TEMs have been constructed using SPICE software. These models serve as a convenient method for analyzing the behavior of the modules and allow for the extraction of model parameters from specifications provided in commercial datasheets [3 - 7]. This approach facilitates the efficient analysis of TEMs and aids in the practical implementation of these devices in various applications.

The combination of mathematical models and SPICE-based equivalent circuit models has proven to be a powerful tool for understanding the characteristics and performance of TEMs. It enables researchers and engineers to conduct in-depth analyses and fine-tune the design of these modules to meet specific requirements and optimize their performance. The thermoelectric effect refers to the generation of an electric field in the opposite direction when a thermal gradient is applied to a solid material. This effect allows thermoelectric materials to be utilized in applications such as refrigeration and electric power generation. The efficiency of a thermoelectric material is quantified by the figure of merit, denoted as Z, as defined in [8].

$$Z= (\sigma^2.\sigma)/k \ .[1/K] \qquad (1)$$

where:

α - material's Seebeck coefficient, V/K,

σ - electrical conductivity of material, S/m,

k – thermal conductivity of material, W/(m.K).

Equation (1) defines the power factor, which is the numerator of the equation. To effectively describe and compare the thermoelectric efficiency and quality of various material systems, the dimensionless figure of merit (ZT) is commonly used. The value of ZT is dependent on the temperature of interest (T), making it a crucial parameter in evaluating thermoelectric materials. Hence, the equation can be reformulated to incorporate ZT as follows:

$$ZT= (\sigma^2.\sigma.T)/k \qquad (2)$$

The key to achieving a high value of ZT lies in two factors: enhancing the power factor (α^2σ) and reducing the thermal conductivity (k). By increasing the power factor, which is a product of the square of the Seebeck coefficient (α) and the electrical conductivity (σ), the thermoelectric material becomes more effective at converting heat into electrical energy. Simultaneously, decreasing the thermal conductivity ensures that the material retains heat more efficiently, minimizing energy loss and maximizing its thermoelectric efficiency. Together, these efforts lead to higher ZT values, making the material more desirable for various practical applications.

A prominent application of thermoelectric technology is for refrigeration purposes. When an electrical current is passed through a material, it induces a temperature difference, which can be harnessed for cooling purposes [8].

2. Principle of thermoelectric module

We are examining a one-dimensional steady-state thermoelectric power generation problem, focusing on a single leg (either n-type or p-type) of the thermoelectric device. The material properties of the thermoelectric material vary with absolute temperature T. In this setup, positive electric current density and heat flux flow from the hot side (Th) to the cold side (Tc). The electric field E and temperature gradient are in the opposite direction of the electric current density J and heat flux Q (see Fig.1). For a simple generator, the electric current density is given by [9].

$$J= I/A \qquad (3)$$

where I is the electric current and A is the cross-sectional area of the thermoelectric element.

In relation to the hot and cold sides, the direction of positive variables is indicated in the illustration. In an efficient generator, with a positive Seebeck coefficient ($\alpha>0$), all variables—electric current (J), electric field (E), and potential (V)—are positive. However, in the case of a negative Seebeck coefficient ($\alpha<0$), these variables (J, E, V) will be negative or opposite to the depicted direction [9].

The electric field in a thermoelectric element is a result of both the reversible Seebeck effect and the irreversible effect governed by Ohm's law. Considering the sign convention mentioned earlier, the electric field originating from a purely resistive element through Ohm's law is expressed as $E = -\rho J$, where ρ represents the electrical resistivity and J is the electric current density.

On the other hand, the electric field arising from the Seebeck effect is given by $E = \alpha \nabla T$, where α denotes the Seebeck coefficient and ∇T represents the temperature gradient. Combining both the Seebeck and Ohm effects, the electric field at any position within the thermoelectric element can be expressed as follows:

$$E= \alpha \nabla T- \rho J \quad (4)$$

Similarly, heat is transported within the thermoelectric element through both the reversible Peltier effect and the irreversible process governed by Fourier's law. The reversible Peltier effect is described by the equation $Q = \alpha TJ$, where αT represents the Peltier coefficient, T is the temperature, and J is the electric current density.

On the other hand, the irreversible heat transport, as per Fourier's law, is given by $Q = k\nabla T$, where k represents the thermal conductivity, and ∇T is the temperature gradient. These two mechanisms combine to govern the overall heat transfer within the thermoelectric element, adhering to the sign convention shown in Figure 1.

$$Q= \alpha TJ+k\nabla T \quad (5)$$

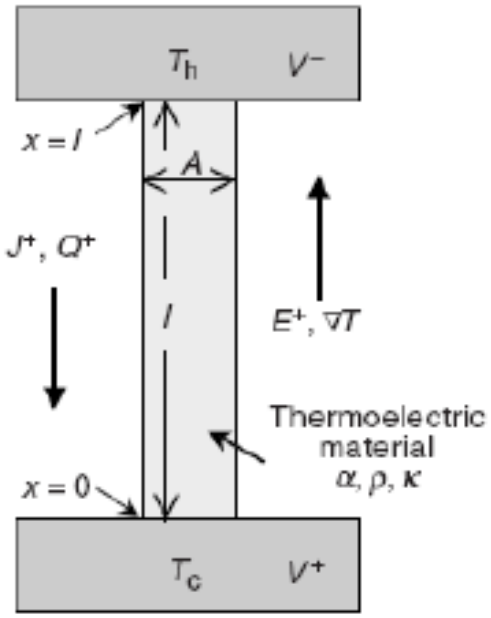

Fig. 1 - Diagram of a single-element thermoelectric generator (Source: [9])

The Peltier effect is commonly regarded as a surface phenomenon occurring between two materials, while the transported heat is a characteristic of a single material [9]. In both Equation 4 and Equation 5, the irreversible and reversible effects are handled separately and can be directly added together. This approach aligns with Kelvin's assumption. Furthermore, the irreversible heat flow is limited by the steady-state heat equation, imposing additional constraints on the overall heat transfer process.

$$\nabla(k\nabla T)= -[T (d\alpha/dT) J\nabla T]- (\rho J^2) \quad (6)$$

where $T (d\alpha/dT)$ is the Thomson coefficient.

The electric power density (P), which represents the power produced per unit volume, is obtained by multiplying the electric field (E) by the electric current density (J).

$$P=EJ \quad (7)$$

Based on the sign convention depicted in Figure 1, a purely resistive element ($\alpha=0$) would necessitate a negative electric field $E = -\rho J$ to generate a positive current (+J), resulting in a negative power density $P = -\rho J^2$ (indicating electric energy consumption).

3. Design Optimization

The efficiency of a thermoelectric generator relies on multiple variables that can be optimized globally to achieve the optimal design. Nonetheless, employing a reduced variable approach in the design problem helps eliminate various interdependencies among design variables. This approach provides a clearer understanding of the impact of each variable in the system [9].

The primary objective of the design process is to assess the maximum achievable thermoelectric efficiency for all temperatures on the hot and cold sides of the thermoelectric generator (excluding the heat sinks). This evaluation leads to an optimized efficiency that solely depends on the thermoelectric hot and cold-side temperatures.

$$\eta = \eta_{max}(Th, Tc) \quad (8)$$

The assumption is that any other variables, such as the chosen materials, interface temperatures, geometry, and current, can be optimized based on given Th and Tc to calculate the efficiency. This holds true for thermoelectric material interface temperatures, but it is less accurate for determining the size of metal interconnect and contact resistance [9].

A. Length of the Thermoelectric Element

After obtaining the optimized efficiency (equation 8) for given Th and Tc, the values of u(T) and Φ(T) are defined for both the n- and p-type elements. Most of the remaining performance parameters also depend on the length of the thermoelectric element. The length (l) is typically determined by the desired total heat flux (Utotal/Atotal) or power per unit area (W/Atotal). To calculate l and establish other operating conditions, the desired total heat flux (Utotal/Atotal) or power per unit area (W/Atotal) must be specified. As a result, the length (l) becomes a function solely of Th, Tc, and Utotal/Atotal.

$$l = l(Th, Tc, Utotal/Atotal) \quad (9)$$

After evaluating the functions in equation (8) and equation (9) for various Th, Tc, and Utotal,h/Atotal values, they can be integrated into the system model to determine the optimal operating conditions for the thermoelectric generator [9]. The power and voltage of the system directly correlate with the size of the generator (determined by Atotal) and the number of thermoelectric couples. After considering all the trade-offs and optimizing the system, the final configuration of the thermoelectric generator can be determined.

B. Voltage

The voltage generated by the system (Vsystem) is equal to the voltage per thermoelectric couple (Vcouple) multiplied by the number of couples connected in series (Nseries) [9].

$$Vsystem = Vcouples \; Vseries \quad (10)$$

Hence, the number of couples connected in series is selected based on the voltage requirement of the system. In many cases, additional parallel circuits (Nparallel) are included to achieve redundancy, ensuring a more reliable thermoelectric generator configuration.

$$Nsystem = Nseries \; Nparallel \quad (11)$$

Once the thermoelectric length is fixed, the total power desired W will define the total cross-sectional area Atotal. The relationship between the area of a couple and the number of couples Nsystem, is given by:

$$Acouple = W/(\{Utotal/Atotal\} \; \eta Nsystem) \quad (12)$$

C. Temperature

Characterization of materials and devices is of paramount importance in thermoelectric research. The composition and various parameters of materials significantly impact the achieved thermoelectric (TE) performance, including functional properties, figure-of-merit, efficiency, coefficient of performance, and sensitivity of the devices. As commonly understood, metals are not ideal thermoelectric materials due to their low Seebeck coefficient and high electron contribution to thermal conductivity (k). Consequently, the electrical conductivity (σ) and thermal conductivity (k) tend to offset each other, resulting in poor thermoelectric performance.

Insulators exhibit a low thermoelectric effect because they possess a high Seebeck coefficient and minimal electron contribution to thermal conductivity, resulting in low charge density and electrical conductivity. On the other hand, semiconductors, which lie between metals and insulators, are considered the most favorable thermoelectric materials [9], [10]. They strike a balance between having a significant thermoelectric effect and desirable electrical conductivity, making them well-suited for thermoelectric applications. The thermoelectric materials selected for the steady-state simulations presented in this paper on a thermoelectric element Peltier cooler are Bismuth-Tellurium (Bi-Te) and Lead-Tellurium (Pb-Te). These materials boast a high Seebeck coefficient (α), a favorable electrical conductivity (σ), and a low thermal conductivity (k), making them ideal choices for efficient thermoelectric applications. In general, the material properties mentioned, such as the Seebeck coefficient, electrical conductivity, and thermal conductivity, can be temperature-dependent and possibly anisotropic. However, in this study, only isotropic material properties are considered, and they are assumed to remain constant throughout the analysis with fixed material parameters.

(Bi,Sb)2(Te,Se)3-based thermoelectric (TE) materials are considered the most promising and predominant choices for cooling applications. Notably, bismuth-tellurium (Bi-Te) and antimony-tellurium (Sb-Te) compounds fall within this category. In recent times, researchers have been exploring nanostructured materials as potential candidates to enhance the performance of thermoelectric devices. Specifically, PbTe nanocomposites have been created using PbTe nanocrystals synthesized through a chemical route, followed by compaction under high pressure and temperature.

Thermoelectric (TE) materials based on (Bi,Sb)2(Te,Se)3 are highly regarded and widely adopted for cooling applications. Notably, compounds such as bismuth-tellurium (Bi-Te) and antimony-tellurium (Sb-Te) are part of this category. Researchers have recently been exploring the use of nanostructured materials to improve the performance of thermoelectric devices. Specifically, PbTe nanocomposites have been developed by synthesizing PbTe nanocrystals through a chemical route, followed by compacting them under high pressure and temperature. These advancements hold great potential for enhancing the efficiency and effectiveness of thermoelectric systems.

4. Evaluation of the Model

A. Heating-Cooling Chamber Simulation

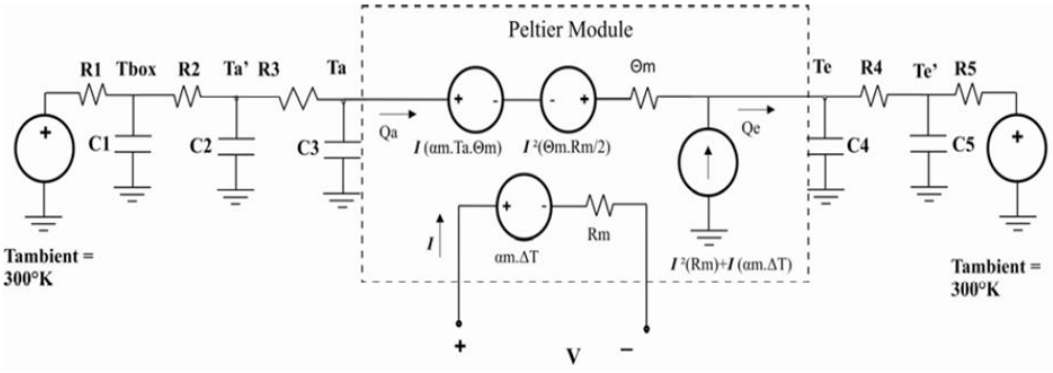

Figure 2. Cooling mode of operation

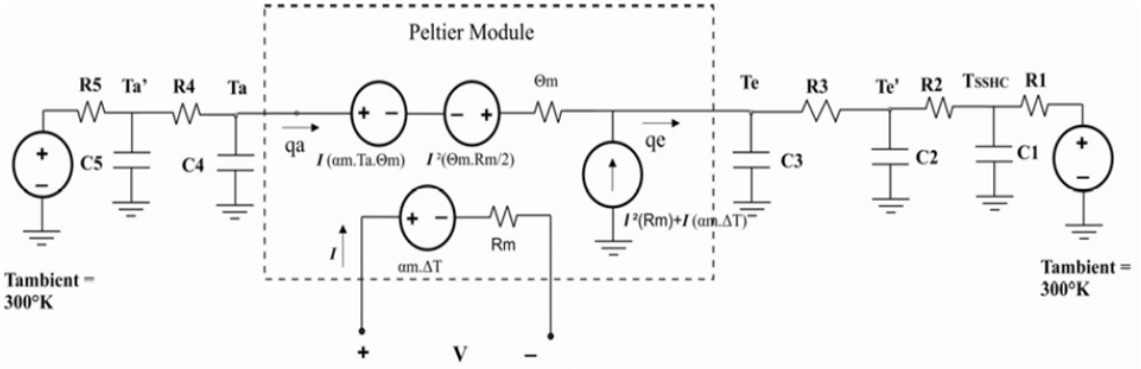

Fig. 3 - Heating mode of operation

The proposed model's equivalent circuit for the Peltier system was successfully implemented in SPICE. Fig. 2 illustrates the cooling mode of operation, while Fig. 3 demonstrates the heating mode of operation. The lumped parameters R's and C's have been defined as follows:

R1: Thermal resistance of the system

R2, R5: Thermal resistance of the het sink + fan

R3, R4: Assembly's thermal resistance

C3, C4: Heat capacity of alumina ceramic plates and pellets of the peltier modules

C2, C5: Heat capacity of the heat sinks

C1: Heat capacity of system

B. Simulation Result

During the cooling process, the temperature will be reduced to 10℃. By using the P-spice software we obtain the graph (fig. 4) as X axis consist of Frequency in Mega Hertz and Y axis consist of Temperature in Kelvin. The voltages used in the simulation are represented by V1, V2, V3, V4 and V5 for supplying 5V for the operation. The current supplied will be 2Amps. During cooling process the resistance R1, R2, R3 will be used for forward operations and the resistance R4, R5 will be used for reverse operations.

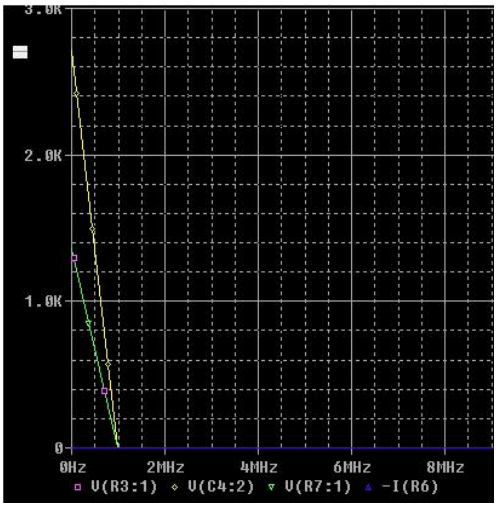

Fig. 4 - Cooling Performance Results

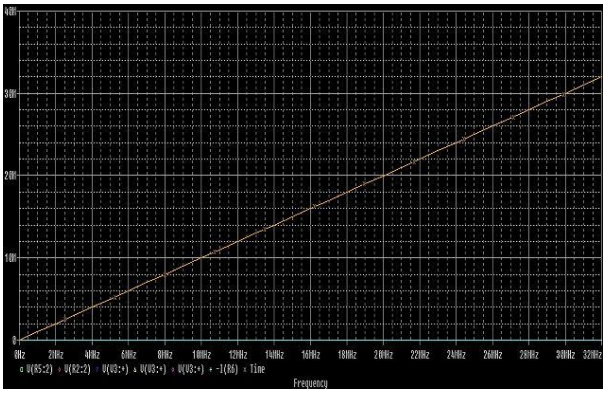

Fig. 5 - Heating performance result

During the heating process, the temperature is gradually increased to 70℃. Using PSpice software, we obtained a graph (Fig. 5) with the X-axis representing Frequency in Mega Hertz and the Y-axis representing Temperature in Kelvin. The simulation involves voltages denoted as V1, V2, V3, V4, and V5, each supplying 5V for the operation. The current supplied during the heating process is 2 Amps. For reverse operations during heating, the resistances R1, R2, and R3 are utilized, while for forward operations, the resistances R4 and R5 come into play.

C. Experimental set-up in Laboratory

The system is initially supplied with 230V, which is then stepped down by the transformer to 12V, 2A, an adequate supply for the Peltier system. To control the Peltier system for both heating and cooling processes, the 89C51 microcontroller is employed, providing easy and efficient control. For the interface between the microcontroller and relay, an opto-coupler is utilized to ensure seamless coupling and reliable operation.

Fig. 6 - Photograph of proposed model

In this setup, two 12V relays are employed to control the direction of current supplied to the semiconductor element, enabling the change in temperature. Temperature sensors sense the variations in temperature, and the analog signals are converted into digital signals using an ADC (Analog-to-Digital Converter). The digital output is then fed into the microcontroller for processing, and the results are displayed. The entire process begins at room temperature, and temperature variations are monitored and recorded in a tabulated format as shown below.

Table 1 – Heating Performance Results

Temp (°C)	32	35	40	45	50	50	55	60	65	68	70
Time (min)	0.45	1.29	2.15	3	3.4	4.5	6	7	7.5	8.4	9.5

Table 2 – Cooling Performance Results

Time (min)	0	1.16	3.15	5.32	6.5
Temp (°C)	28	25	20	17	15

D. Experimental Result

The graph (Fig. 7) represents the results of the heating process, with time on the x-axis and temperature on the y-axis. The hot process begins at room temperature and gradually increases the temperature over time, reaching a maximum of 70°C at 9.5 minutes. Intermediate readings are recorded and presented in the table above (Table 1).

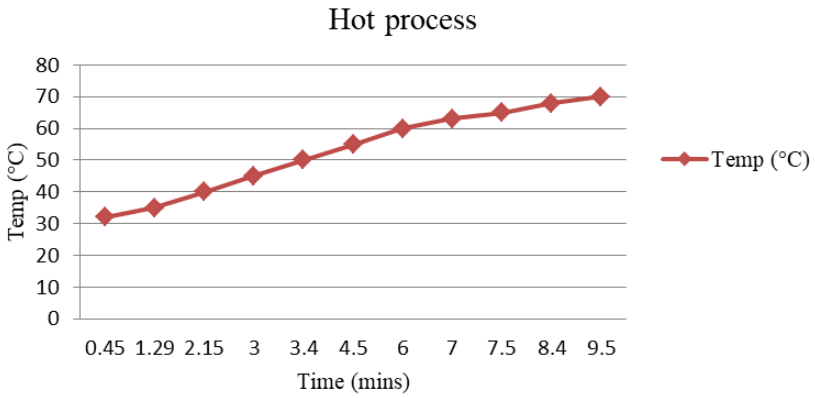

Fig. 7 - Hot Process Result

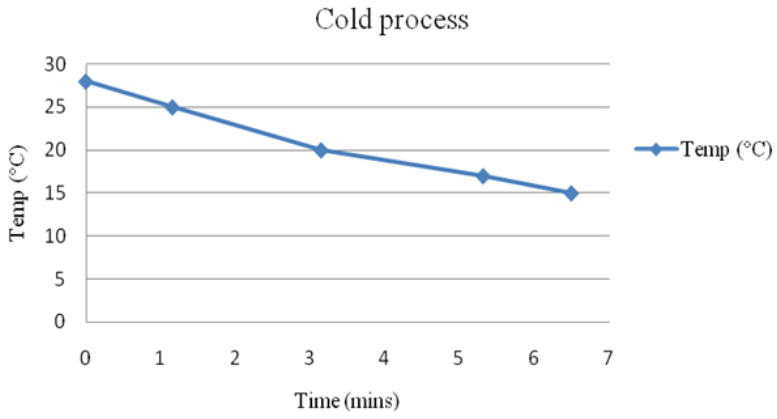

Fig. 8 - Cold Process Result

The graph (Fig. 8) depicts the results of the cooling process, with time on the x-axis and temperature on the y-axis. The cold process begins at room temperature and steadily decreases the temperature over time, reaching a minimum of 15°C at 6.5 minutes. Intermediate readings are recorded and presented in the table above (Table 2).

Table 3 – Comparison Table

Time (min)	Hot Temperature (°C)	Cold Temperature (°C)
0	30	70
0.45	32	60
1.29	35	55
2.15	40	50
3	45	40
3.4	50	38
4.5	55	36
5	57	35
6	60	30
7	63	28
7.5	65	26
8.4	68	24
9.5	70	20
14		15
17		13

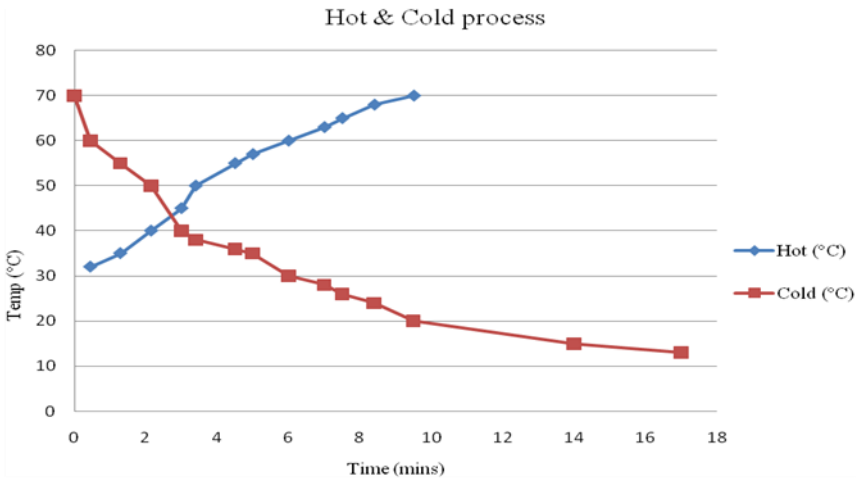

Fig. 9 - Comparison of Hot and Cold process

The typical procedure involves initiating the hot process at room temperature. Consequently, the temperature gradually rises with time until it reaches 70°C; this takes approximately 9.5 minutes (see Fig. 9). Once the target temperature of 70°C is achieved, the freezing process is initiated by pressing the cold button, leading to a gradual decrease in temperature. It takes approximately 14 minutes to reach a temperature of 15°C. Various intermediate readings are recorded and presented in the table above (Table 3).

5. Conclusions

A comprehensive model was developed to simulate the Peltier thermoelectric module. To validate this model, a heating and cooling chamber was designed and fabricated, incorporating Peltier modules. The model employs controlled sources and lumped parameters, making it highly compatible for simulation with software like Spice. The entire system was rigorously tested and simulated using Spice, encompassing various input current values. Remarkably, the simulation results exhibited a close match with the experimental data. Furthermore, this model is easily expandable, as lumped parameters R's and C's can be incorporated to represent the thermal resistance and heat capacities of a thermal system, enabling its simulation in Spice. Recorded and presented in the table above (Table 3).

REFERENCES

Devijoti Pal, Ali Ansari, Kantanu Kr. Behera, A Report on Design & Setup of Peltier Module Based Air Cooler, *IEEE Trans. Instrum. Meas*. pp.54, 1548 (2020)

Subhash Sahu, Satish Prajapati, Abhishek Bhandari, An Experimental Study of Sustainable Cooling using Peltier Effect *IEEE Trans. Ind. Appl*. 43, pp.505 (2020).

Ankur Mishra, Manoj Kumar, Peltier Thermoelectric Cooling Module, International Journal of Recent Technology and Engineering, Vol. 9, pp.208–212, 2020

A.F. Ioffe, *Semiconductor Thermoelements and Thermoelectric Cooling* (London, UK: Infoserch Limited, 1957).

S.W. Angrist, *Direct Energy Conversion* (Boston: Allyn and Bacon, 1982), pp. 177.

J.A. Cha´vez, J.A. Ortega, J. Salazar, A. Turo´, and M.J. Garcı´a, *IEEEIMTC.* pp. 2, 1019 (2000).

S. Lineykin and S. Ben-Yaakov, *IEEE Power Electron*. Lett. 3, pp.63 (2005).

D. Mitrani, J.A. Tome´, J. Salazar, A. Turo´ , M.J. Garcı´a, and J.A. Cha´vez, *IEEE Trans. Instrum. Meas*. pp.54, 1548 (2005).

M. Chen, L.A. Rosendahl, I. Bach, T. Condra, and J.K. Pedersen, *Int. Conf. Thermoelect*, pp.214 (2006).

S. Lineykin and S. Ben-Yaakov, *IEEE Trans. Ind. Appl*. 43, pp.505 (2007).

Kimmel, J. – *Thermoelectric Materials*, Physics 152, Special Topics Paper, March 2, 1999

D.M. Rowe, Ph.D., D.Sc., *Thermoelectric Handbook Macro to Nano*, 2006 by Taylor & Francis Group, LLC

H. Julian Goldsmid, *Introduction to Thermoelectricity*, Springer Series in Materials Science, 2009.

Biplab Paul and Pallab Banerji - *Grain Structure Induced Thermoelectric Properties in PbTe* Nanocomposites, Nanoscience and Nanotechnology Letters, Vol. 1, pp.208–212, 2009

Zhuomin M. Zhang, *Nano/Microscale Heat Transfer*, Mc Grow Hill, 2007.

Acshayden , and K-Qiu (2011) "Peltier Thermoelectric Modules Modeling and Evaluation" Journal of Electronic materials,Vol.40, No.5, pp.606-610.

Alaoui Chakib (2009) "Peltier Thermoelectric Modules Modelling and Evaluation" International journal of Engineering (IJE), Vol.5, pp.114-121.

Alaoui.C and Salameh.Z, (July 2011) "Solid State Heater Cooler: Design and Evaluation" Large Engineering Systems Conference on power engineering.